Determination of Electroweak Parameters

Seminar 'Particle Physics at the LHC'
Proceedings

R. Gugel

Freiburg, 27.05.2014

Contents

1 Motivation

The Standard Model of particle physics describes interactions between particles which are considered to be the elemental constituents of the (visible) matter in the universe. One important sector of the Standard Model is the electroweak sector with the gauge bosons γ, $W^{\pm}$ and Z^0.

Todays electroweak theory is the result of the unification of electromagnetic interactions with the weak interaction. Before the unification by Glashow, Salam and Weinberg in 1961, there were two distinct types of interactions: The electromagnetic interaction mediated by the photon (γ) - which is not only well known in high energy physics, but also in low energy physics - and the weak interaction, first known from the decay of heavy nuclei through charged currents. Before the electroweak unification the weak interaction was described by the Fermi theory, assuming a point interaction and later by the V-A-theory including the parity violation observed for example in the Wu-experiment in 1956 [13]. The theoretical structure of the electroweak interaction is $SU(2)_L \times U(1)_Y$ yielding four fields called W_1, W_2, W_3 and B. However, these fields emerging from demanding gauge invariance under $SU(2)_L \times U(1)_Y$ transformations are not the physically observable fields, which are given by linear combinations of the theoretical fields: W_1 and W_2 are combined to the two orthogonal fields $W^{\pm} = \frac{1}{\sqrt{2}}(W_1 \mp iW_2)$, representing the charged currents in the electroweak theory. W_3 and B form the photon field $A = B\cos\theta_W + W_3 \sin\theta_W$, where θ_W is the so called *weak mixing angle* or *Weinberg angle*. After identifying $W^{\pm}$ and A as the known physical fields, we are left with a fourth orthogonal combination $Z = -B\sin\theta_W + W_3\cos\theta_W$ predicting a new gauge boson called Z^0. While the photon couples only to the the electric charge, the $W^{\pm}$ and Z^0 also couple to electrically neutral particles such as neutrinos. First evidence for the existence of a weak, neutral current was found at CERN in 1973 in bubble chamber experiments through $\nu_\mu e$ scattering [14].

Around 1965 the Higgs, Brout, Engler and others added the BEH-mechanism to the theory giving $W^{\pm}$ and Z^0 bosons a mass while leaving the photon massless, in consistency with experimental measurements. The BEH-mechanism introduces a new particle, known as the Higgs particle discovered in 2012 at the Large Hadron Collider (LHC) by the ATLAS and CMS experiments [15], [16]. The discovery of the Higgs boson and the measurement of its mass allows for the first time to overconstrain the electroweak theory and test its validity.

Some of the basic relations between the parameters of the electroweak modell are at

Born level:

$$\begin{aligned} e = g\sin\theta_W = g'\cos\theta_W, \quad & m_W = m_Z\cos\theta_W, \\ G_F = \frac{\sqrt{2}g^2}{8m_W^2}, \quad & \alpha = \frac{e^2}{4\pi}, \\ m_H = v\sqrt{2\lambda} = \frac{\sqrt{8\lambda}m_W}{g} & \end{aligned} \tag{1.1}$$

where g and g' are the coupling strengths of fermions to the $SU(2)_L$ and the $U(1)_Y$ part of the electroweak theory respectively. G_F is the Fermi constant, m_W, m_Z and m_H are the masses of the $W^\pm$, Z^0 and Higgs bosons. The relations in eq. (1.1) allow to choose four independent parameters and thereby fixing all others. A usual choice is $G_F, \sin\theta_W, m_W$ and m_H. Higher orders in pertubation theory give rise to additional relations. Examples for higher order corrections to the mass of the W boson are shown in fig. 1.1. While the Higgs loop correction to the mass of the W boson is $\sim \log m_H/m_W$, the correction due to the quark loops is $\sim (m_u - m_d)^2$, where $m_{u/d}$ is the mass of the quarks in the loop, making the $t\bar{b}$ loop the dominating one of the quark loop corrections.

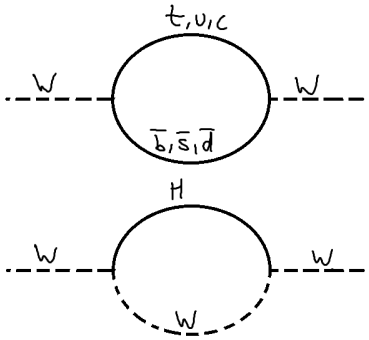

Figure 1.1: *Feynman diagrams showing loop corrections to the mass of the W boson. While the diagram with the Higgs boson results in a contribution $\sim \log m_H/m_W$, the quark loop results in a correction $\sim \Delta m^2$, where Δm is the mass difference of the quarks involved and therefor dominated by the term $\sim (m_t - m_b)^2$*

Before the discovery of a new particle in 2012, which is now considered a Higgs boson, precise measurements of the masses of the W boson and the top quark allowed to impose constraints on the mass of a Standard Model Higgs boson, excluding mass regions which had not been excluded yet by direct searches (c.f. fig. 1.2).

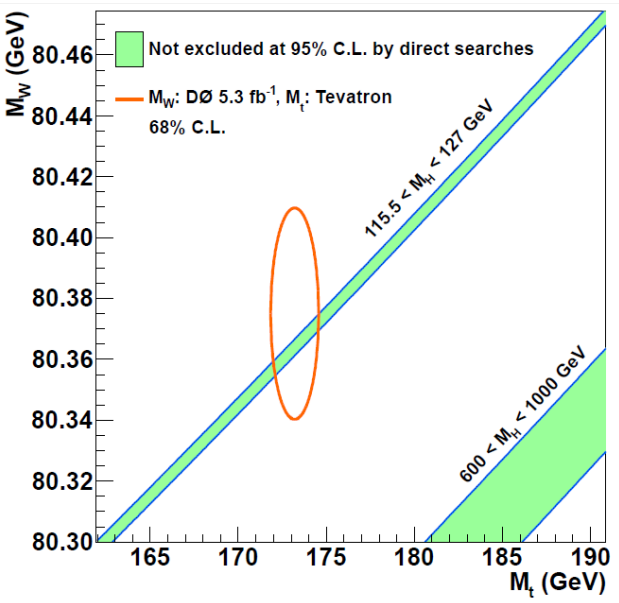

Figure 1.2: m_W *and* m_t *measurement results with exclusions on* m_H *from direct searches (from ref. [1])*

2 Template Method

Collider experiments usually do not allow for direct calculation of theoretical parameters from the measured data. The template method allows to measure parameters using event simulations for a finite number of assumed parameter values without limiting the possible results to values used in the simulations. Given a physics parameter m is to be measured, using theoretical predictions one produces distributions in some observable d (for example transverse momentum p_T, transverse mass m_T or missing transverse energy E_T^{miss}) for different values of m each. In the next step an arbitrary function f with parameters p_j is fitted to the simulated distributions in the (m, d)-plane, determining values for the parameters p_j. This function is then used to determine the physics parameter m by fitting the obtained function to distributions in d obtained from data, fixing the p_j to the values extracted from the fit to simulations and allowing m to be varied. An example for simulations using diffrent m_t values is shown in fig. 2.1

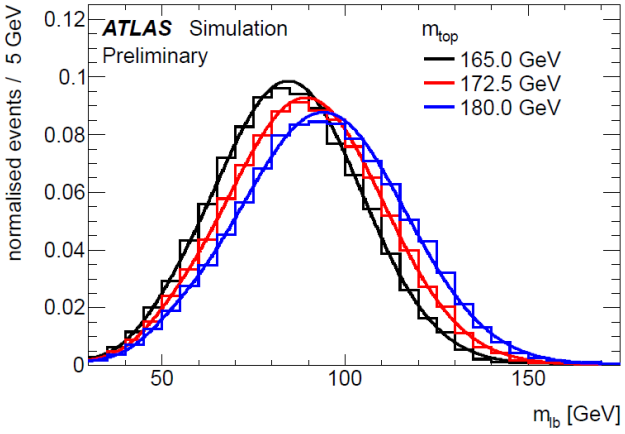

Figure 2.1: *Example for simulated distributions for the template method (from ref. [4])*

3 Mass of the W Boson

W bosons are produced at hadron colliders mainly through $q\bar{q}' \to W + X$, where X represents hadronic recoil and gluon initial state radiation (ISR). For precise measurements the decay channel $W \to \ell\nu$ is used, where the lepton ℓ is restricted to be an electron or muon, resulting in a branching ratio of $\approx 22\%$. The exclusion of tau leptons is due to the fact that tau leptons decay within the detector producing one ($\tau \to \nu_\tau + q\bar{q}'$) or two additional neutrinos ($\tau \to \nu_\tau + \bar{\nu}_\ell\ell$) preventing a precise measurement. In addition the hadronically decaying τ leptons are hard to distinguish from other hadronic activity in the detector (e.g. underlying event). In order to be as independent as possible from theoretical models, the analyses presented in the following measure m_W using kinematic distributions: The template method is applied using distributions in p_T^ℓ, m_T and E_T^{miss}:

$$\begin{aligned} p_T^\ell &= p^\ell \cos\theta \\ m_T &= \sqrt{2p_T^\ell p_T^\nu (1 - \cos\Delta\phi)} \\ E_T^{\text{miss}} &= \left| \sum_{i \in \text{event}} \vec{p}_T^{\,i} \right| = p_T^\nu \end{aligned}$$

3.1 Measurement at the D0 Detector (2012)

The mass of the W boson was measured at the D0 detector using $4.3\ \text{fb}^{-1}$ of $\sqrt{s} = 1.96\ \text{TeV}$ data recorded at the Tevatron collider at Fermi National Accelerator Laboratory (Fermilab) [1]. For the analysis only the $W \to e\nu$ decay channel was used.

In order to achieve a high precision measurement, a precise calibration of the electromagnetic and hadronic calorimeter is required. To this end, the precisely known mass of the Z boson $m_Z = 91\ 188 \pm 2\ \text{MeV}$ [3] is used. For the electromagnetic calorimeter it is assumed that the measured energy E^{meas} is given by

$$E^{\text{meas}} = \alpha E^{\text{true}} + \beta.$$

The values for α and β are determined through fits to $Z \to ee$ events in the invariant mass m_{ee}, the electron energy E_e and electron angular distributions. The hadronic calorimeter is then calibrated using η_{imb} the projection of $\vec{p}_T^{\,ee} + \vec{u}_T$ onto the axis parallel to $\vec{e}^{\,\ell_1} + \vec{e}^{\,\ell_2}$. $\vec{u}_T$ is the (transverse) vectorial sum over all energy deposits except for $\vec{p}_T^{\,ee}$. A comparison of data and simulation of the dielectron invariant mass spectrum is shown in fig. 3.1.

For the $W \to e\nu$ event selection the requirements $p_T^e > 25\ \text{GeV}$, $E_T^{\text{miss}} > 25\ \text{GeV}$ as well as $u_T < 15\ \text{GeV}$ and $m_T \in (50, 200)\ \text{GeV}$ are imposed, demanding significant transverse momentum of the electron (p_T^e) and the neutrino (E_T^{miss}), small

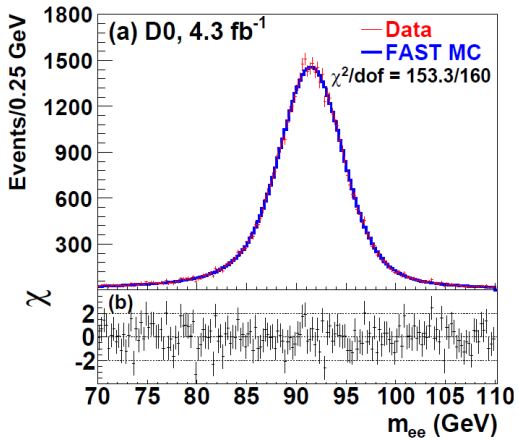

Figure 3.1: *Comparison of data and simulation of the dielectron invariant mass spectrum at the D0 detector (from [1])*

hadronic recoil (u_T) and a reasonable transverse mass for a W boson decaying in the transverse plane. The distributions of data and the fitted theoretical predictions in m_T and p_T^e are shown in fig. 3.2. In addition the template method was also used for distributions in E_T^{miss}, however this part of the analysis does not contribute to the combined result. The combined result is

$$m_{W,\text{D0}} = 80.367 \pm 0.013(\text{stat.}) \pm 0.022(\text{syst.}) \text{ GeV}$$

This resulting uncertainty is clearly dominated by systematic uncertainties. A list of

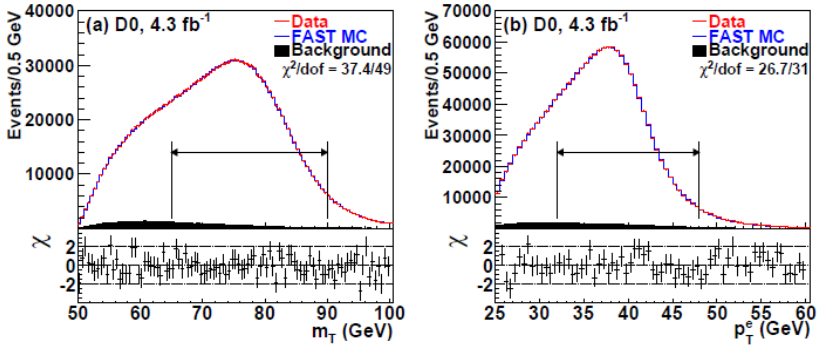

Figure 3.2: *Data and template fit for m_T and p_T^e distributions in $W \to e\nu$ events at the D0 detector (from [1])*

the contributions to the systematic uncertainty is shown in fig. 3.3. The most important contributions are the calibration of the electron energy and for the E_T^{miss} analysis also the modelling of the hadronic recoil on the experimental side and uncertainties on the parton density functions on the theoretical side.

TABLE II: Systematic uncertainties of the M_W measurement.

Source	ΔM_W (MeV) m_T	p_T^e	$\not{E}_T$
Electron energy calibration	16	17	16
Electron resolution model	2	2	3
Electron shower modeling	4	6	7
Electron energy loss model	4	4	4
Hadronic recoil model	5	6	14
Electron efficiencies	1	3	5
Backgrounds	2	2	2
Experimental subtotal	18	20	24
PDF	11	11	14
QED	7	7	9
Boson p_T	2	5	2
Production subtotal	13	14	17
Total	22	24	29

Figure 3.3: *List of systematic uncertainties in the measurement of the mass of the W boson at D0. The leading contributions have been highlighted (from [1])*

3.2 Measurement at the CDF Detector (2013)

The second detector at the Tevatron collider that measured the mass of the W boson is the Collider Detector Fermilab (CDF). In the referenced analysis compared to D0 only data corresponding to an intergrated luminosity of 2.2 fb^{-1} at $\sqrt{s} = 1.96$ TeV has been used. In contrast to the D0 analysis the CDF analysis also includes the $W \to \mu\nu$ decay channel.

The momentum scale of the detector was calibrated using the well known resonances J/ψ and Υ, decaying into two muons. The calibration was achieved through a comparison of simulations with data. An energy scale calibration was extracted by means of a likelihood fit to the peak in the E/p distribution in $Z \to ee$ decays.

The kinematic variables used in the CDF analysis are essentially the same variables as in the D0 analysis. As an example the m_T distribution in the $W \to \mu\nu$ channel is shown in fig. 3.4

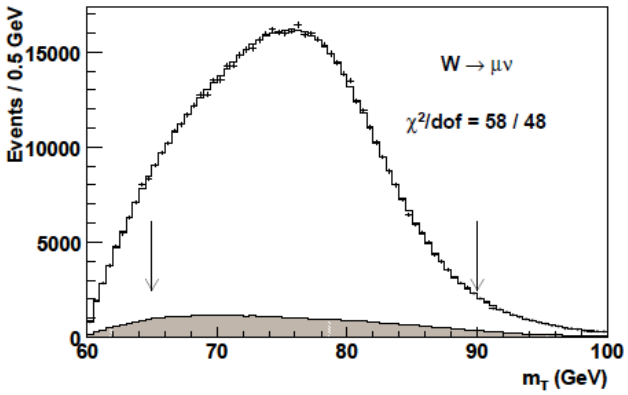

Figure 3.4: *m_T distribution for the $W \to \mu\nu$ channel at the CDF detector. The arrows indicate the range used for the fit to data in the template method, the shaded area is the background contribution extracted from the fit. (from [2])*

The CDF analysis achieves smaller systematic uncertainties for the lepton energy scale, however the systematic uncertainties from hadronic recoil and PDFs are similar to the D0 analysis. A list of sources of systematic uncertainties for the m_T fit is shown in fig. 3.5. The systematic uncertainty of the combined result is therefor comparable to the statistic uncertainty

$$m_{W,\mathrm{CDF}} = 80.387 \pm 0.012(\mathrm{stat.}) \pm 0.015(\mathrm{syst.})\ \mathrm{GeV}$$

Taking correlations between different experiments into account, the world average,

	m_T fit uncertainties		
Source	$W \to \mu\nu$	$W \to e\nu$	Common
Lepton energy scale	7	10	5
Lepton energy resolution	1	4	0
Lepton efficiency	0	0	0
Lepton tower removal	2	3	2
Recoil scale	5	5	5
Recoil resolution	7	7	7
Backgrounds	3	4	0
PDFs	10	10	10
W boson p_T	3	3	3
Photon radiation	4	4	4
Statistical	16	19	0
Total	23	26	15

Figure 3.5: *Systematic uncertainties in the CDF m_T based analysis (from [2])*

including earlier measurements at Tevatron and at LEP, is

$$m_W = 80.385 \pm 0.015\ \mathrm{GeV}$$

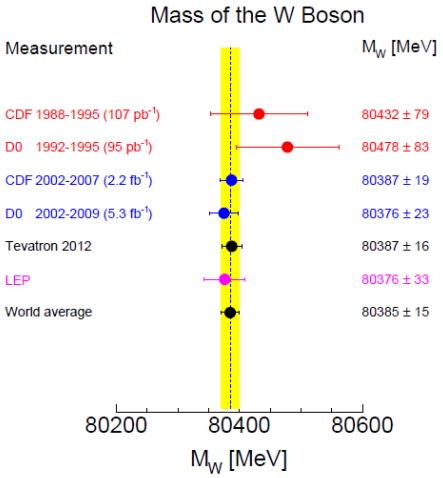

Figure 3.6: *Comparison of different results for m_W with combined values for Tevatron and world average (from [3])*

4 Mass of the Top Quark

Top quarks are the only quarks known with a life time below the time scale for hadronization. This makes top quarks the only quarks whose mass can be measured at collider experiments in an unconfined state (i.e. before hadronization). The dominant decay channel of top quarks is $t \to bW$, where the analyses of $t\bar{t}$ events are usually subdivided depending on the decay mode of the W bosons. The leptonic decay of both W bosons $WW \to \ell\nu\ell'\nu'$ (dilep) occurs with a branching ratio of about 4% (again excluding the decay to τ leptons), the semileptonic decay $WW \to \ell\nu q\bar{q}'$ (lep+jets) features a branching ratio of about 29% and the third decay channel used for analyses where both W bosons decay hadronically (all jets) has a branching ratio of about 45%. The most important step in the event selection is the so called *b-tagging*, assigning a tag to jets originating from a b quark in $t \to bW$ decays. For the ATLAS detector this is accomplished with a neural network exploiting the topology of the t decay. The working point is chosen at an efficiency of 70% for the tagging of b-jets, yielding a mistagging rate of about 1 in 130 light quark jets.

4.1 Analysis in the Dilepton Channel at ATLAS

The analysis presented in ref. [4] uses data corresponding to $4.7\ \mathrm{fb}^{-1}$ of $\sqrt{s} = 7\ \mathrm{TeV}$ collisions recorded by the ATLAS detector at the LHC. The event selection requires exactly 2 b-tagged jets, high E_T^{miss}, exactly 2 oppositely charged leptons and at least two jets in the central detector region, each with $p_T > 25\ \mathrm{GeV}$. This strict event selection strongly suppresses the main backgrounds originating from $Z \to \ell^+\ell^-$ and associated (single) top production (see fig. 4.1)

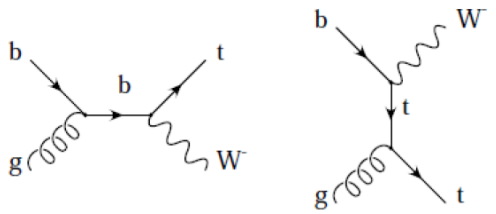

Figure 4.1: *Leading order Feynman diagrams for the associated production of a t quark and a W boson (from ref. [12])*

To determine the mass of the top quark, the template method is used with a kinematic variable called $m_{\ell b}$ which is defined as follows: For each event there are two possible combinations to match a lepton to a b-jet, each combination allowing to calculate two invariant masses, the invariant mass of the matched lepton and b-jet system as well as the invariant mass of the remaining $\ell + b$-jet cobination. For each combination the average of the two invariant masses is calculated, defining $m_{\ell b}$ as the lower one of the

resulting two averaged invariant masses. The simulated event distribution in $m_{\ell b}$ is shown in fig. 2.1 for different assumptions of m_t. The fit to data is shown in fig. 4.2, resulting in

$$m_{t,\mathrm{dilep}} = 173.09 \pm 0.64(\mathrm{stat.})\ \mathrm{GeV}$$

with the quoted uncertainty being the statistical uncertainty obtained from the fit. Leading systematic uncertainties originate from the modelling of hadronization and underlying event on the theoretical side and from (b-)jet energy scale as well as b-tagging on the experimental side, leading to a systematic uncertainty of $1.5\ \mathrm{GeV}$.

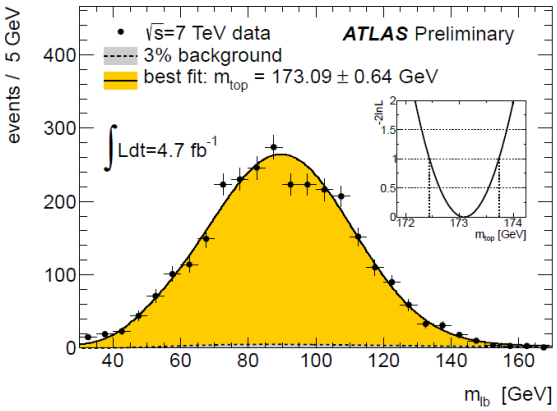

Figure 4.2: *Template fit to data in the ATLAS dilep analysis for the mass of the top quark (from ref. [4])*

4.2 Analysis in the Lep+Jets Channel at ATLAS

The lep+jets decay channel of a $t\bar{t}$ pair features advantages compared to the other decay channels, making it the most precise channel for the measurement of the mass of the top quark. In contrast to the dilep channel it allows for full reconstruction, since only one neutrino is involved[1]. This allows to actually reconstruct an invariant mass of possible top quark systems. The all jets channel imposes difficulties in terms of combinatorics: While the lep+jets channel only has two independent matching combinations (if exactly four jets are present, assign either of the b-jets to the two light jets originating from the hadronically decaying W boson), the all jets channel produces four jets from light quarks where any combination of two light quarks jets can be matched to one of the b-jets.

The ATLAS analysis presented in ref. [5] uses data corresponding to $1.04\ \mathrm{fb}^{-1}$ of $\sqrt{s} = 7\ \mathrm{TeV}$ colissions. The event selection requires two b-tagged jets, at least least four jets in the central detector region, each with $p_T > 25\ \mathrm{GeV}$ as well as exactly one

[1] In case there is only one neutrino involved in the event its transverse momentum can be assumed to be the missing transverse momentum. If one assumes furthermore that the W boson from which the neutrino originated was on-shell, i.e. fulfilling $E^2 = p^2 + m_W^2$, even the longitudinal momentum of the neutrino can be (roughly) reconstructed.

lepton and $E_T^{\text{miss}} > 20$ GeV[2]. The analysis is subdivided into two subanalyses using different analysis methods.

4.2.1 1D-Analysis

The 1d-analysis applies the template method in one dimension (i.e. as presented in section 2). The variable used is

$$R_{32} = \frac{m_{\text{top}}^{\text{reco}}}{m_W^{\text{reco}}}$$

where m_i^{reco} is the reconstructed invariant mass of the hadronically decaying top quark and the corresponding W boson respectively. Using such a ratio leads to a (partial) cancellation of uncertainties of energy scales. For the matching of the two light quark jets to a b-tagged jet a likelihood fit is performed for each event using the event kinematics, choosing the combination with the highest likelihood to calculate R_{32}. The likelihood used is a product of transfer functions of energy deposits and momenta associated with the event, Breit-Wigner functions for the reconstructed W and t candidates as well as a weight introducing information from the b-tagging. The otained distribution together with the theoretical prediction is shown in fig. 4.3

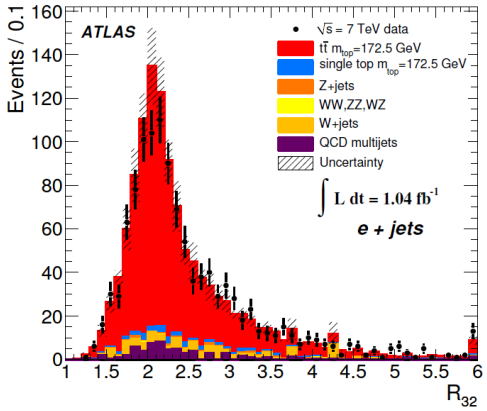

Figure 4.3: *R_{32} distribution of data and simulation in the ATLAS 1d-analysis of lep+jets channel (from [5])*

4.2.2 2D-Analysis

The 2d-analysis also uses the template method to measure the mass of the top quark, however instead of using a distribution in one variable, the analysis uses the event distribution in the $(m_{\text{top}}^{\text{reco}}, m_W^{\text{reco}})$-plane. The (hadronic) top quark candidate is chosen from the set of b + two light jet triplets by selecting the one with the highest transverse momentum, with the restriction that the invariant mass of the light jet system is between $50 - 110$ GeV. The free fit parameters in the template fit are m_t, JSF (jet energy scale factor) as well as n_{bkg} (number of background events). Instead of reducing

[2]The exact event requirements are slightly different for the cases where the lepton is an electron or a muon as well as for the different subanalyses. The full event requirements are listed in ref. [5]

the impact of the systematic uncertainty due to jet energy scaling as in the 1d-analysis, the jet energy scaling is performed *in situ*. Thereby the 2d-analysis reduces the systematic uncertainty at the cost of increasing the statistic uncertainty due to the lower number of events in each bin in the $(m_{\text{top}}^{\text{reco}}, m_W^{\text{reco}})$-plane (compared to bins in R_{32}).

The results of the subanalyses are

$$m_{t,1d} = 174.4 \pm 0.9(\text{stat.}) \pm 2.5(\text{syst.}) \text{ Gev} \qquad m_{t,2d} = 174.5 \pm 0.6(\text{stat.}) \pm 2.3(\text{syst.}) \text{ GeV}$$

The correlation between these two results is quoted in ref. [5] to be below 50% due to different jet triplet selection and estimators for m_{top}. A breakdown of uncertainties is shown in fig. 4.4, the combined result does not contain contributions from the 1d-analysis. Hence the result fo the 2d-analysis is quoted as the final result.

	1d-analysis		2d-analysis		Combinations		Correlation
	e+jets	μ+jets	e+jets	μ+jets	1d	2d	ρ
Measured value of m_{top}	172.93	175.54	174.30	175.01	174.35	174.53	
Data statistics	1.46	1.13	0.83	0.74	0.91	0.61	
Jet energy scale factor	na	na	0.59	0.51	na	0.43	0
Method calibration	0.07	< 0.05	0.10	< 0.05	< 0.05	0.07	0
Signal MC generator	0.81	0.69	0.39	0.22	0.74	0.33	1
Hadronisation	0.33	0.52	0.20	0.06	0.43	0.15	1
Pileup	< 0.05	< 0.05	< 0.05	< 0.05	< 0.05	< 0.05	1
Underlying event	0.06	0.10	0.42	0.96	0.08	0.59	1
Colour reconnection	0.47	0.74	0.32	1.04	0.62	0.55	1
ISR and FSR (signal only)	1.45	1.40	1.04	0.95	1.42	1.01	1
Proton PDF	0.22	0.09	0.10	0.10	0.15	0.10	1
W+jets background normalisation	0.16	0.19	0.34	0.44	0.18	0.37	1
W+jets background shape	0.11	0.18	0.07	0.22	0.15	0.12	1
QCD multijet background normalisation	0.07	< 0.05	0.25	0.33	< 0.05	0.20	(1)
QCD multijet background shape	0.14	0.12	0.38	0.30	0.09	0.27	(1)
Jet energy scale	1.21	1.25	0.63	0.71	1.23	0.66	1
b-jet energy scale	1.09	1.21	1.61	1.53	1.16	1.58	1
b-tagging efficiency and mistag rate	0.21	0.13	0.31	0.26	0.17	0.29	1
Jet energy resolution	0.34	0.38	0.07	0.07	0.36	0.07	1
Jet reconstruction efficiency	0.08	0.11	< 0.05	< 0.05	0.10	< 0.05	1
Missing transverse momentum	< 0.05	< 0.05	0.12	0.16	< 0.05	0.13	1
Total systematic uncertainty	2.46	2.56	2.31	2.57	2.50	2.31	
Total uncertainty	2.86	2.80	2.46	2.68	2.66	2.39	

Figure 4.4: *Breakdown of uncertainties in the ATLAS lep+jets analysis. A correlation quoted as* (1) *means full correlation between the analyses for each lepton channel, but no correlation between different lepton channels. (from [5])*

A comparison of results from different experiments and analysis channels is shown in fig. 4.5, showing good consistency between the different results.

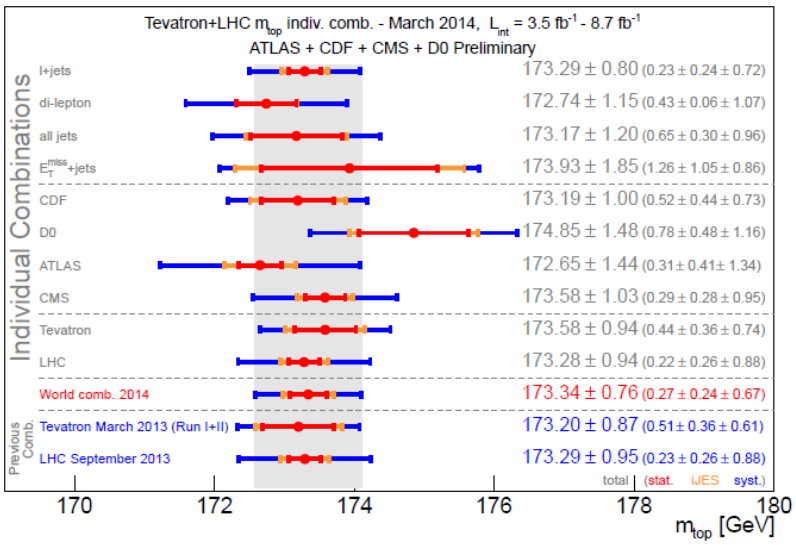

Figure 4.5: *Comparison of m_t measurements and analysis channels. (from [7])*

5 Test of the Standard Model

In order to test the consistency of the electroweak sector of the Standard Model a global fit has been performed in ref. [9], assuming that the boson found around 125 GeV at the LHC in 2012 is the Standard Model Higgs boson. A comparison of the m_t fit with experimental results is shown in fig. 5.1. The fit included 19 parameters out of which five were freely varying leading to 14 degrees of freedom. In order to obtain a measure for the consistency of the Standard Model, the χ^2 of the fit is compared to a χ^2 distribution for 14 degrees of freedom shown in fig. 5.2. In order to validate the assumption of a χ^2 distribution, a set of toy analyses is constructed by allowing the experimental results to vary within their uncertainties. The resulting probability (p-value) for the Standard Model describing the physical processes correctly is around 8% depending on whether theoretical uncertainties are included or not.

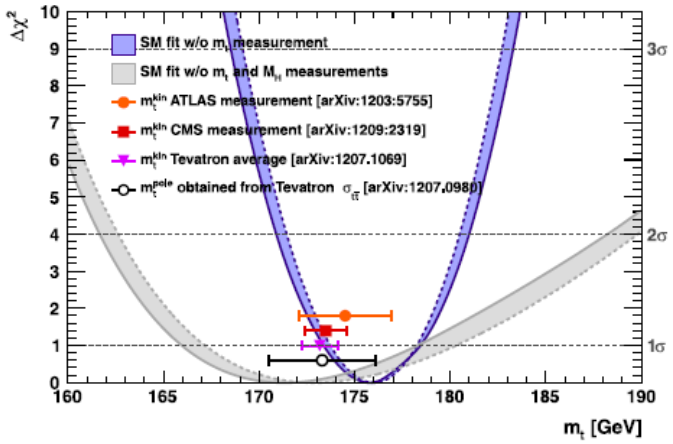

Figure 5.1: $\Delta\chi^2$ *of the electroweak fit as a function of* m_t *with experimental results for comparison (from [9])*

While the motivation for precise measurements of m_W and m_t before the discovery of the Higgs boson was mainly to find exclusions on m_H, the focus has since changed: In fig. 5.3 the predicted m_W values as a function of m_t are shown for the particle around 125 GeV being the Standard Model Higgs boson or a (heavy, CP even) Higgs boson in a MSSM. As can clearly be seen from the plot, it is not yet possible to exclude any of the two possibilities. The experimental uncertainties of both m_t and m_W are dominated by systematic uncertainties. Despite the absolute uncertainty of m_t being by far larger than the uncertainty of m_W, for an exclusion of either of the two theories an improvement in the m_W accuracy is required. Due to the limitation by systematic uncertainties this imposes a huge challenge for future experiments and analyses.

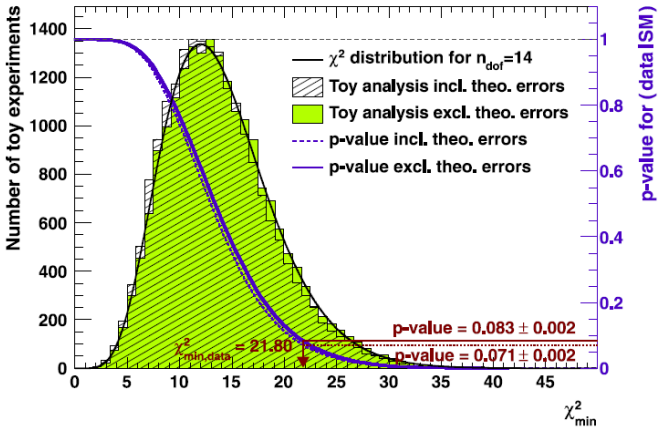

Figure 5.2: χ^2 *distribution for 14 degrees of freedom together with the probability for encountering a* χ^2 *value larger than a certain value and toy analyses validating the assumption of a* χ^2 *distribution*

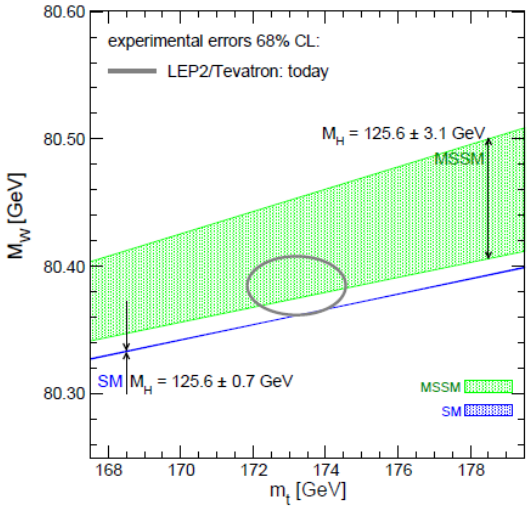

Figure 5.3: *Comparison of regions for* m_W *and* m_t *in case of one Standard Modell (SM) Higgs boson and in case of the Higgs boson being one of the Higgs bosons in a minimal super symetric model (MSSM). The width of the MSSM band is due to additional parameters in the MSSM (from [11])*

Bibliography

[1] D0 Collaboration, *Measurement of the W Boson Mass with the D0 Detector*, arXiv:1203.0293v2, 14. Apr 2012

[2] CDF Collaboration, *A precise measurement of the W-boson mass with the Collider Detector Fermilab*, arXiv:1311.0894v2, 29 Apr 2014

[3] CDF Collaboration, D0 Collaboration, *Combination of CDF and D0 W-Boson Mass Measurements*, arXiv:1307.7627v2, 1 Aug 2013

[4] ATLAS Collaboration, *Measurement of the Top Quark Mass in Deleptonic Top Quark Pair Decays with $\sqrt{s} = 7$ TeV ATLAS Data*, ATLAS-CONF-2013-077, 18 July 2013

[5] ATLAS COllaboration, *Measurement of the Top Quark Mass with the Template Method in the $t\bar{t} \rightarrow$ lepton+jets Channel using ATLAS Data*, arXiv:1203.5755v2, 12 Jun 2012

[6] ATLAS Collaboration, CMS Collaboration, *Combination of ALTAS and CMS results on the mass of the top-quark using up to $4.9\ \mathrm{fb}^{-1}$ of $\sqrt{s} = 7$ TeV LHC data*, ATLAS-CONF-2013-102, 18 Sep 2013

[7] ATLAS, CDF, CMS and D0 Collaborations, *First combination of Tevatron and LHC measurements of the top-quark mass*, arXiv:1403.4427v1, 18 Mar 2014

[8] ALTAS Collaboration, *Measurement of the mass difference between top and anti-top quarks in pp collisions at $\sqrt{s} = 7$ TeV using the ATLAS detector*, arXiv:1310.6527v3, 9 Dec 2013

[9] Gfitter Group, *The electroweak fit of the standard model after the discovery of a new boson at the LHC*, Eur. Phys. J. C (2012) 72:2205, 3 Nov 2012

[10] A.Pich, IFIC, University of València - CSIC, *The Standard Model of Electroweak Interactions*, arXiv:1201.0537v1, 2 Jan 2012

[11] S.Heinemeyer et al., *Implications of LHC search results on the W boson mass prediction in the MSSM*, arXiv:1311.1663v1, 7 Nov 2013

[12] ATLAS Collaboration, *Evidence for the associated production of a W boson and a top quark in ATLAS at $\sqrt{s} = 7$ TeV*, arXiv:1205.5764v2, 16 Aug 2012

[13] Wu, C. S. and Ambler, E. and Hayward, R. W. and Hoppes, D. D. and Hudson, R. P., *Experimental Test of Parity Conservation in Beta Decay*, PhysRev.105.1413, Feb. 1957

[14] F. J. Hasert *et al.*, *Search for Elastic Muon-Neutrino Electron Scattering*, Phys. Lett. B 46 121-124

[15] ATLAS Collaboration, *Observation of a new particle in the search for the Standard Model Higgs boson with the ATLAS detector at LHC*, arXiv:1207.7214, 31 Jul 2012

[16] CMS Collaboration, *Observation of a new boson at a mass of 125 GeV with the CMS experiment at the LHC*, arXiv:1207.7235, 31 Jul 2012